CHEMO-HYGRAL AND PORO-MECHANICAL MODELING FOR ASR AND STRUCTURAL PERFORMANCE ASSESSMENT OF RC BRIDGE DECKS

Yuya Takahashi[1]*, Yasushi Tanaka[1], Koichi Maekawa[1]

[1]The University of Tokyo, Tokyo, JAPAN

Abstract

This study aims to assess the impacts of alkali silica reaction (ASR) on the fatigue lives of reinforced concrete slabs used in bridge decks. The authors have been developing a 3D multi-scale computational platform to trace the chemical and physical events in structural concrete. Anisotropy rooted in migration and expansion of ASR substances in both micro-pores and crack gaps is modelled based upon the scheme of poro-mechanics. The developed models are applied to the fatigue life assessment of RC bridge decks. Previous experimental works on moving-wheel-type loading for bridge decks is referred for experimental verification. It is confirmed that the models introduced in this study may bring about fair behavioural simulation. Furthermore, both experiments and analyses indicate that ASR does not always cause unfavourable structural performances of RC slabs under repeated traffic loads, but it might have led to some extension of fatigue life. The proposed model also promotes the study on so called disintegration of concrete composites owing to the cyclic pore-pressure provoked by the fatigue loading.

Keywords: alkali silica reaction, poro-mechanics, fatigue life, bridge deck

1 INTRODUCTION

The alkali silica reaction (ASR) is one of the major deteriorations of concrete composites and its modelling has been studied by many researchers [1-5]. Saouma [1] is developing FEM models for ASR in consideration of micro-chemical reactions and trying to apply the models to the structural levels. Multon et al. [2] is also developing the analytical model to consider the anisotropic expansion with ASR. Furthermore, some practical methods to simulate structural performances of ASR deteriorated concrete are being investigated to solve its complexity of solid concrete and ASR gel's kinematics inside pores. Especially for multi-directionally reinforced conditions, simple empirical formulas might be out of its applicable ranges.

Meanwhile, the authors are developing multi-scale chemo-hygral computational system, DuCOM-COM3 [6], which can conduct 3D multi-scale analysis of structural concrete. Based on above-mentioned background, the authors have been developing a model for ASR reaction and its mechanistic actions accompanying multi-directional cracking [7,8] on the scheme of Biot's solid-liquid two-phase interaction model [9] and non-orthogonal crack-to-crack interaction modelling [10]. In this study, the developed system is applied to the structural concrete. Fatigue life of RC bridge slabs exposed to ASR is targeted and experimentally verified with the past engineering experiences and facts. The coupled complex effect of condensed water, drying shrinkage and ASR on fatigue performance is further investigated with the analytical studies.

2 MODELLING OF ASR-INDUCED EXPANSION AND CRACKS

2.1 ASR-gel generation model

The proposed ASR-induced expansion model is being built on the basis of poro-mechanics [8], which has been used in geotechnical engineering applications such as consolidation and liquefaction of soil foundation. The ASR-gel is treated as the medium existing among crack spaces and micro-voids. Figure 1 shows the modelling of ASR-gel creation and their contribution on the expansion. Based on the chemical equations (a), (b) for ASR, the rate of ASR is formulated as a function of alkali concentration, free water and the reactive aggregate's contents expressed by Eq. (c). The coefficient of reaction rate "k" is set to 0.1×10^{-7} by the inverse sensitivity analyses, and the effects of relative humidity (RH) and temperature are also taken into account in Eq. (d) and Eq. (e). The generated ASR-gel volume is calculated by assuming $X_2Si_2O_5(H_2O)_{8.4}$ as the ASR gel molecular formula for each

* Correspondence to: takahashi@concrete.t.u-tokyo.ac.jp

alkali, X (X is Na or K)[11]; the consumed alkali and water are also calculated in terms of mass conservation. It is a point of the theorem that water and alkali contents in pore solution, which are control parameters for computing the reaction rate, are set forth as global variables of both the thermodynamic analytical system (DuCOM) and the 3D meso-scale structural analytical system (COM3). In the scheme of DuCOM, the multi-ionic approach developed by Elakneswaran et al. [12, 13] is used to compute the mass balances of sodium and potassium. Through this composition of mass and momentum conservation, the strong coupling between the material properties and the mechanical phenomena is realized in life-simulation of structural concrete.

On the basis of generated gel volume, stress formation can be calculated. Here, some part of created gels can contribute to the stress formations but the rest of it does not. The gel is partially absorbed into the capillary pores [14] and the amounts of absorbed gel can be calculated by Eq. (j), which is the function of the gel pressure. The rest of gels may substantially contribute to the stress formations. Regarding the gel-oriented internal pressure, the authors consider the semiliquid characteristics of ASR-gels. In order to express the solid-liquid coexisting states, parameter β is introduced, which is the ratio of the solid phase to total ASR-gel. In the case of certain stress conditions, the solidified part of produced ASR-gel can expand uniformly even under anisotropic pressure distribution as Eq. (l), while the liquefied part expands without shear rigidity under the isotropic pressure expressed by Eq. (m). The total pressure can be computed as the sum of those partial pressure components as Eq. (k). Parameter β is tentatively assumed to be 0.2 for the first assumption with sensitivity analysis. The volumetric stiffness of ASR gel is supposed to be the same as the one of condensed water tentatively.

2.2 Reduced crack width with ASR gel for shear transfer

Produced gel volume and the pressure defined on the gel phase are given the constitutive model of concrete skeletons as intermediate variables. Almost all formulae are the same as those of no-ASR concrete [10], but for the shear transfer model alone, we have to consider the existence of ASR-gel products staying in between crack planes, because the shear stress can be transferred through the ASR substances as well. It is proposed that an equivalent reduced crack width according to the crack filling ratio of ASR-gel is used in the contact density model [10], as shown in following equation.

$$\delta' = \left(1 - k * R_{asr}\right) \cdot \delta$$

with: δ': reduced crack width
k: reduction factor (determined as 0.7)
R_{asr}: ASR-gel filling ratio in crack
δ: crack width

The reduction factor denoted by k is assumed to be 0.7 from the inverse sensitivity analyses, and it means that ASR-gel in cracks has resistivity against shear force and partially contributes to shear transfer between cracks.

2.3 Disintegration model

In the fatigue simulation of concrete composites with condensed water, mean stiffness degradation accompanying disintegration of aggregate-cement paste system is influential in the long term performance [15]. When the micro-pore pressure raises, it may provoke the local pressure developing near aggregates' surface, where capillary pores of rather large sizes are concentrated. Then, the cyclic pore pressure in this interfacial zones will produce the debonding between aggregate and cement paste matrix. This degradation is thought to be mechanically similar to the freeze-thaw actions, although the physical and mechanical driving forces differ.

In reference to the past research on freezing-thawing cycles, the reduction parameter K is expressed by the pore water pressure path history Z (initial value is 0) in a differential form with respect to pore water pressure p as;

$$Z = \int_{path} dZ$$

$$dZ = -10^{n} \cdot \left(1 + f_n\right) \cdot p_{ampl}{}^{f_n} \cdot dp$$

$$K = \exp\left(-Z\right)$$

with: f_n and n: coefficients related to the inclination and section of the S-N curve
p_{ampl}: amplitude of pore water pressure

With the disintegration, the bond of reinforcement and concrete is also lost. When disintegration progresses completely, K becomes 0. Then, reinforcing bars may also lose transverse stability like reinforcing bars arranged close to concrete covers of seismic resistant members. It is assumed that the load bearing capacity against axial compression would also deteriorate similar to the buckled rebars in columns under seismic actions when structural concrete is disintegrated as;

$$\sigma_i = K \cdot \sigma_{ci} + \sqrt{K} \cdot \sigma_{si} + (1 - K) \cdot \sigma_{agg}$$

with: σ_{ci}: stress allocated to concrete part

σ_{si}: stress allocated to steel part

σ_{agg}: stress with aggregate assembly

With disintegration in progress, cement paste can be eroded and stress allocated to concrete part will be decreased and finally comes to zero when *K* becomes zero. But, even in such a condition, aggregate assembly can stand against the volumetric contraction like the soil foundation. The third term in right-hand side of the equation express the effect of aggregate assembly having no binder of cement paste. Stress with aggregate assembly is calculated supposing that the stiffness of the assembly is almost 1/100 of normal concrete. With this composite model, it is considered that high pressurized water in cracks may accelerate the deterioration of the slabs with fatigue loads.

3 FATIGUE LIFE SIMULATION OF RC BRIDGE SLABS

3.1 Experiments in past research

RC slabs in bridge decks, whose thicknesses are generally small compared to span length, receive the direct load from vehicles. Hence, it leads to the deterioration of the slab members due to moving fatigue loads. In some northern districts in Japan, serious deteriorations of bridge slabs are reported, especially because of the severe cold climate and anti-freezing agents sprayed every winter. Anti-freezing agents, which contains high alkali, can accelerate ASR deteriorations, too. The combination of ASR, stagnant water laid on the bridges and high cycle moving loads has great impact to the degradations of structural performances. To know the long-term performance of such RC slabs, coupled effects of those factors should be investigated.

Maeshima et al. [16, 17] conducted valuable experimental studies on the fatigue life of slabs of the real scale specimens using a wheel-type loading machine as shown in Figure 2. For studying the effect of ASR on the fatigue life, they prepared four RC slabs in the same dimensions and exposed to the several conditions of ASR acceleration [17, 18]. Figure 3 shows shapes and dimensions of RC slab specimens. The specimens were made as double layer reinforced RC slabs with the size of 3000mm×2000mm×160mm and the span length is 1800mm. Cover depth of the top and bottom faces are both 30mm. Main reinforcement bars are arranged in 150mm intervals while distributing bars are arranged in 120mm intervals.

Table 1 shows the mix proportion of concrete used. The gravel is reactive of ASR and additional sodium chloride is included to mixture to accelerate ASR. Three different levels of ASR expansions are prepared; Case I is no ASR acceleration case as a reference, Case II has 41days of ASR acceleration (50°C, RH80%, saturated sodium chloride solution is kept on the upper surface of the slab, as shown in Figure 4) and expansion of 2800μ in the vertical (in the direction of the thickness of slabs) and 800μ in the horizontal (longitudoinal along the reinforcement) directions came up. Case III has the environmental conditions of 87 days in 5% sodium chloride solutions and 59 days of ASR acceleration. Expansive strains of Case III reached 4900μ in the vertical and 700μ in the horizontal directions. The compressive strength of concrete is 25.5MPa for Case I specimen at 34 days, 34.3MPa for Case II at 97 days, and 34.6MPa for Case III at 177 days.

Moving load was applied to those RC slab specimens. The standard load is 98kN according to the actual traffics, and after designated cycles of loading passages, the load was increased in stages of 29.4kN of increment. Only in Case III, condensed water was supplied on the surface of the slab as shown in Figure 5 during loading to see the effect of stagnant water on fatigue life. Finally, loading cycles are converted to the equivalent cycles of standard load (98kN) by assuming the Miner's empirical law.

Figure 6 shows the results of Maeshima's experiments [18]. Though the live load deflection at the first cycle in ASR case (Case II) is larger than no-ASR case (Case I), the fatigue life is one-order (10 times) longer in the ASR case than the non-ASR. It was mentioned that chemical pre-stress can partly restrain the increase in live load's deflections. And the effect of water is not so significant in the ASR cases when we see the result of Case II and Case III, although it is known that the existence of water generally reduces fatigue life dramatically in the no-ASR concrete cases [7, 15]. After the test of case III, disintegration of the concrete composites can be observed on the slab like Figure 7, it is the result of cyclic high water pressure.

3.2 Analytical study for the experimental results

The experiment described in the previous section was tried to be simulated with the proposed models. Analytical FE discretization is prepared as shown in Figure 8. Taking advantage of symmetry, only halves of the slabs are numerically modelled. The same supporting conditions are set forth and the constant 98kN is numerically applied for the moving loads. For the no-ASR case, to examine the effect of shrinkage, simulations with and without drying shrinkage of concrete were conducted. The free shrinkage strain was simply introduced as a free volumetric one before loading with the linear gradient from 500μ at the top and bottom surfaces to 0μ at the centre of the slab. For ASR cases, 300μ of free ASR expansions were induced in 100 days before the loading step. As a result, expansions are about 3,000μ in the transverse vertical direction and about 800μ in the in-plane horizontal directions due to the confinement by the dispersed reinforcing bars. In ASR cases, shrinkage is not considered because water was always supplied in ASR acceleration conditions.

Figure 9 shows both the absolute and live load deflections at the mid-span of the slabs along cyclic moving loads. For the absolute deflection, the value is calculated as {(total deflection) – (residual deflection at first loading step)}. We can see that shrinkage surely affects the stiffness of RC slabs in non-ASR case because of the shrinkage cracking. The deflection at the first cycle is about half of the experimental value without shrinkage, whereas it is almost the same as the experiment with shrinkage. It is thought that the shrinkage due to drying might occur in Case I specimen. If we see the analytical results of live load deflection, a similar trend with experiment can be observed. The deflection at the first cycle is larger in the ASR case than the no-ASR, but the deflection of the no-ASR case exceeds the ASR-cases after about million cycles. Here, the applicability of the proposed models to the structural scale seems to be confirmed; for the specimen size, the applicability was already shown in previous study [8]. If we see both absolute total and live load deflections, the fatigue life is not so different with and without ASR. From these analytical and experimental studies, it can be suggested that ASR has some beneficial impact on the structural performance of RC slabs as well as damages, although the critical impacts to the structural performances have been reported in previous studies such as rupture of bent reinforcing bars [19].

The effect of water existence is not significant in simulations as seen in experiments, comparing Case II and Case III. As mentioned before, it is commonly known that water existing in the cracks reduces the fatigue lives of bridge slabs. However, in both experiments and analyses shown in this chapter, water doesn't affect much to the fatigue life when ASR is occurred in the RC slab. The combined effect of ASR cracks and water should be studied.

3.3 Effect of water on fatigue lives of bridge slabs

In the previous section, it was interestingly shown that ASR deterioration might reduce the damages caused by water on the fatigue lives of bridge slabs. Also drying shrinkage surely affects to the structural performance of bridge slabs. It is important to see the coupled effect of those factors (ASR, drying shrinkage and stagnant water), herein an analytical study is conducted in this section.

Table 2 shows the series of simulations. Totally eight simulations are conducted to examine each effect of ASR, drying shrinkage and water, individually. Analytical conditions other than these factors are the same as those of the previous section. Figure 10 indicates the simulated mid-span deflections of these cases. We can see the various effects of a sole factor on the fatigue behaviours.

With ASR expansion and cracks, fatigue lives are not so significantly changed, while the deflection, which corresponds to the remaining stiffness, becomes larger. Cracks due to ASR expansion can reduce the stiffness and the fatigue life of RC slabs, but at the same time, chemically induced pre-stress forces of compression can resist against the excessive deformation. As a result, fatigue life is not so changed compared to the non-ASR conditions. Figure 11 shows the strain distribution of the noASR-noSH-DRY case and the ASR-noSH-DRY at one million cycles of loading. For the figure for the ASR case, the initial strain induced by ASR expansion is extracted, so strain only due to loading action is displayed in the figure. The cracking is seen to be widely distributed on the slab and the load carrying mechanism deviates from that of the no ASR case. It should be here mentioned that presence of water causes little difference on fatigue life just in the ASR-noSH case (see Figure 10(c)). Meanwhile, drying shrinkage has great impact to the fatigue life. It can be seen from the figures that occurrence of shrinkage before loading increases the deflection of the slabs and fatigue life reduction with water. The fatigue life reduction due to water is around one-order in noASR-noSH case (Figure 10(a)), while 2 to 3 order reduction happens in the shrinkage cases (Figure 10(b) and Figure 10(d)). From these calculations, ASR seems to reduce the effect of water on fatigue life whereas the drying shrinkage plays a negative role on it. In between these contradictory effects, the negative effect with the drying shrinkage is supposed to exceed the opposite effect of ASR.

To see the effect of water, disintegration of concrete composite is clearly reproduced in the simulations. As mentioned in section 2.3, serious disintegration is predicted to proceed in the case of water conditions and it has large effects on the long-tern fatigue performance as well. The deterioration parameter *K* is calculated as an index of disintegration so that we can discuss the degree of disintegration with this *K* value. Figures 12-15 show the contour maps of *K* value with principal strain distributions for four water existing cases. Contours at two different loading cycles (ten thousands, one-million) are illustrated in the figures. The initial value of *K* is 1.0, which means no reduction of stiffness and strength in terms of disintegration. With the highly cyclic pore water pressure, K decreases gradually and finally goes to 0.0. The value of *K* at the certain point stands for the water pressure history at that point.

We can see from the figures that the degree of disintegration progresses gradually with the increase in number of cycles on the loading area as well as the range of disintegration enlarges. Here, we can see the significant behaviours in the ASR-noSH case. No reduction of *K* can be observed until 10000 cycles, and even at 1E+6 cycles, degree of disintegration is small. Figure 16 shows *K* parameter changes at the point of the top surface of the mid-span (point A in Figure 8), which is most severe point regarding the disintegration. Only in the ASR-noSH case, the *K* value keeps 1.0 until around 1E+5 cycles. This little disintegration is supposed to be the cause of little effect of water on fatigue life on RC slab. The little disintegration means that pore water pressure in cracks has not risen so much. It can be understandable that cracks due to ASR-induced expansion is large enough to release the water pressure caused by cyclic loadings, while other cracks (i.e. cracks caused by shrinkage) hold water in cracks and high water pressure accelerate the disintegration. In shrinkage cases, the area of disintegration is larger than no shrinkage cases and this might cause the large water effect on the fatigue life reduction. With these analytical studies, we can know that not all cracks has negative effect on the fatigue performance of RC slabs.

4 CONCLUSIONS

This study aims to assess the effects of the alkali silica reaction (ASR) on the fatigue lives of reinforced concrete slabs used in bridge decks. Models for ASR-induced expansion and cracks were introduced first. Anisotropy attributed to migration and expansion of ASR substances in pores and crack gaps were modelled on the basis of multi-phase poro-mechanics and the equivalent crack width for the shear transfer along cracks with ASR gels is newly introduced. The developed models are applied to the evaluation of structural performance of ASR degradation. The fatigue lives of RC slabs experimented in previous studies are simulated for the verifications and the similar trend to the reality in experiments is obtained in the simulation tool. From both experiments and analyses, it is indicated that ASR is generally the defect of materials but in some cases, it may bring about favourable effects in structural engineering viewpoint. Chemically induced pre-stress forces in compression to cracked concrete may elevate the capacity which compensates the damage of cracking by ASR expansion, and it may lead to the easy drainage of water which consequently reduces the pore-pressure. As a result, it is shown in both experiments and analyses that water doesn't affect much to the fatigue life when ASR is occurred in the RC slab. The combined effect of ASR cracks and water should be studied in future. It is also realized that drying shrinkage of concrete and pre-induced cracking can accelerate the disintegration and has large impact to the fatigue performance due to the easy penetration of condensed water. With these analytical studies, we can know that not all cracks has negative effect on the fatigue performance of RC slabs.

5 REFERENCES

[1] Saouma, V. E. (2014): Numerical Modeling of AAR, CRC press.

[2] Multon, S., Sellier, A. and Cyr, M. (2009): Chemo-mechanical modeling for prediction of alkali silica reaction (ASR) expansion, Cement and Concrete Research, (39):490-500.

[3] Bažant, Z. P. and Steffens, A. (2000): Mathematical model for kinetics of alkali-silica reaction in concrete, Cement and Concrete Research, (30): 419-428.

[4] Bangert, F., Kuhl, D. and Meschke, G. (2004): Chemo-hygro-mechanical modelling and numerical simulation of concrete deterioration caused by alkali-silica reaction, International Journal for Numerical and Analytical Methods in Geomechanics, (28): 689-714.

[5] J. Liaudat, A. Martínez, C. López, I. Carol (2015): Numerical Modelling of ASR Expansion in Concrete, Proceedings of CONCREEP10: 445-454.

[6] Maekawa, K., Ishida, T. and Kishi, T. (2008): Multi-Scale Modeling of Structural Concrete, Taylor and Francis.

[7] Meakawa, K. and Fujiyama, C. (2013): Rate-dependent model of structural concrete

incorporating kinematics of ambient water subjected to high-cycle loads, Engineering Computations, 30(6): 825-841.
[8] Takahashi, Y., Shibata, K. and Maekawa, K. (2014): Chemo-hygral modeling and structural behaviors of reinforced concrete damaged by alkali silica reaction, Proceedings of ACF2014: 1274-1281.
[9] Biot, M. A. (1963): Theory of stability and consolidation of a porous media under initial stress, Journal of Mathematics and Mechanics, 12(2): 521-541.
[10] Maekawa, K., Pimanmas, A. and Okamura, H. (2003): Nonlinear Mechanics of Reinforced Concrete, Taylor & Francis.
[11] Ichikawa, T. and Miura, M. (2007): Modified model of alkali silica reaction, Cement and Concrete Research (37): 1291-1297.
[12] Elakneswaran, Y. and Ishida, T. (2014): Development and Verification of an Integrated Physicochemical and Geochemical Modelling Framework for Performance Assessment of Cement-Based Materials, Journal of Advanced Concrete Technology (12): 111-126.
[13] Elakneswaran, Y. and Ishida, T. (2013): Integrating physicochemical and geochemical aspects for development of a multi-scale modeling framework to performance assessment of cementitious materials, Multi-scale Modeling and Characterization of Infrastructure Materials, RILEM BOOKSERIES (8): 63-78.
[14] Muranaka, M. and Tanaka, Y. (2013): Development of physical and chemical model for concrete expansion due to ASR based on reaction mechanism, Journal of JSCE, E2/V-69, (1): 1-15.
[15] Hiratsuka, Y., Maekawa, K. (2015): Multi-scale and multi-chemo-physics analysis applied to fatigue life assessment of strengthened bridge decks, Proceedings of XIII International Conference on Computational Plasticity. Fundamentals and Applications: 596-607.
[16] Maeshima, T., Koda, Y., Tsuchiya, S., Iwaki, I. (2014): Influence of corrosion of rebars caused by chloride induced deterioration of fatigue resistance in RC road bridge deck, Journal of JSCE, 70(2): 208-225.
[17] Goto, T., Kishira, T., Ono, A., Maeshima, T. (2014):Wheel-type moving load test for bridge slabs using reactive coarse aggregates, Proceedings of Road bridge slab symposium, (8).
[18] Maeshima, T., Koda, Y., Iwaki, I., Ota, K., Ono, A., Kishi. Y. and Kubo, Z. (2014) Fatigue resistance assessments of RC bridge decks deteriorated by ASR, Proceedings of JSCE (69): 1221-1222 (in Japanese).
[19] Japan Society of Civil Engineers (2005): Concrete Library 124, State-of-the-Art Report on the Countermeasures for the Damage Due to Alkali-Silica Reaction :I26-I31.

ACKNOWLEDGEMENTS

This study was financially supported by JSPS KAKENHI Grant No. 15H05531 and Cross-ministerial Strategic Innovation Promotion Program (SIP).

TABLE 1: Mix proportion.

W/C (%)	Air (%)	s/a (%)	Unit weight (kg/m^3)					Admixture (C×%)		NaCl (kg/m^3)
			W	C	S1	S2	G	AD	AE	
65.0	4.5±1.5	45.0	175	269	413	405	1032	1.5	0.06	18.9

TABLE 2: Simulation series.

Series	ASR expansion	Shrinkage	Water
noASR-noSH-dry	0μ	0μ	Not existing
noASR-noSH-wet	0μ	0μ	Existing
noASR-SH-dry	0μ	500μ at surface, 0μ at center	Not existing
noASR-SH-wet	0μ	500μ at surface, 0μ at center	Existing
ASR-noSH-dry	300m in free expansion	0μ	Not existing
ASR-noSH-wet	300m in free expansion	0μ	Existing
ASR-SH-dry	300m in free expansion	500μ at surface, 0μ at center	Not existing
ASR-SH-wet	300m in free expansion	500μ at surface, 0μ at center	Existing

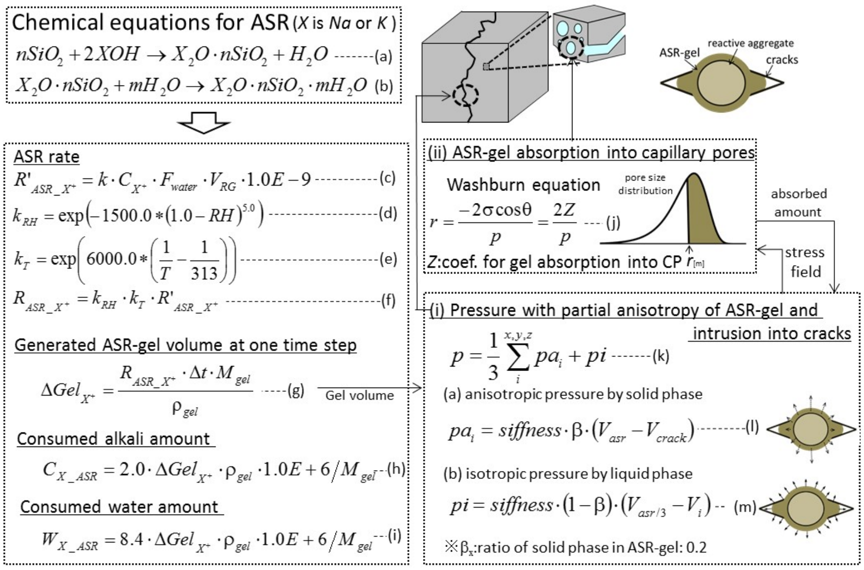

FIGURE 1: Chemical and Physical models for ASR

FIGURE 2: Moving load fatigue test machine [16]

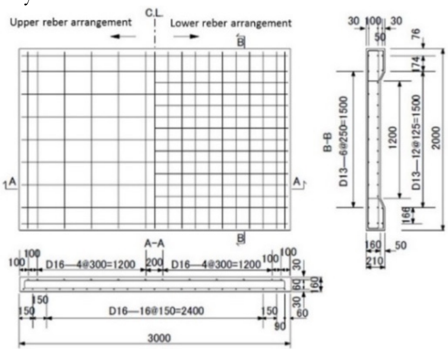

FIGURE 3: ASR acceleration condition [17]

FIGURE 4: The shape of experimented RC slabs [17]

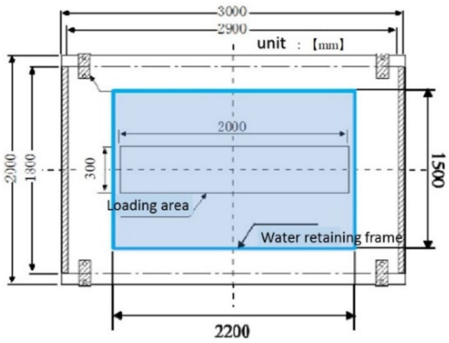

FIGURE 5: Water retaining area for Case III [17]

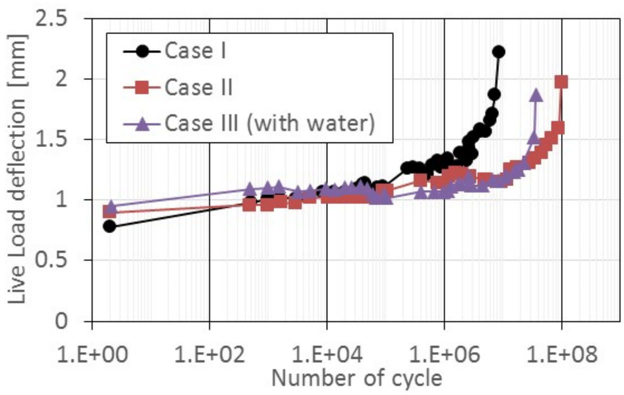

FIGURE 6: Experimental results of moving load tests of RC slabs [17]

FIGURE 7: Appearance of disintegration

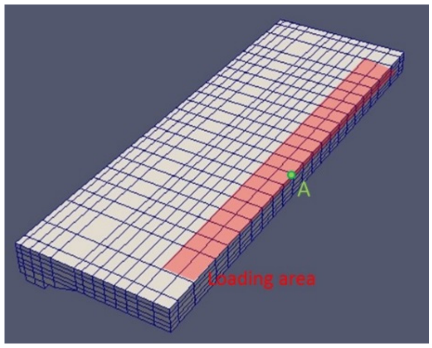

FIGURE 8: Analytical mesh

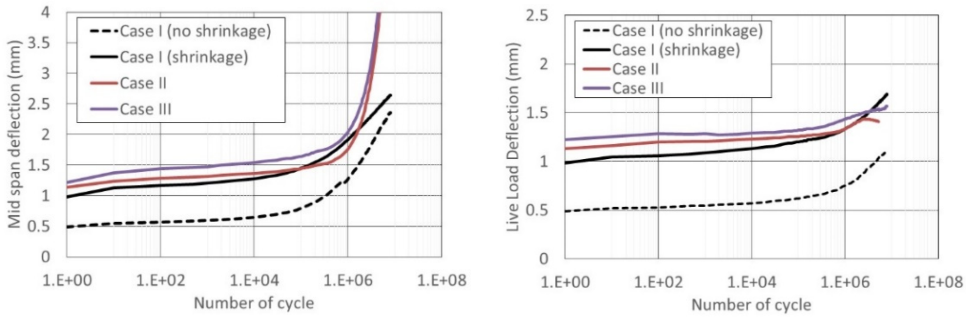

FIGURE 9: Analytical results with proposed models

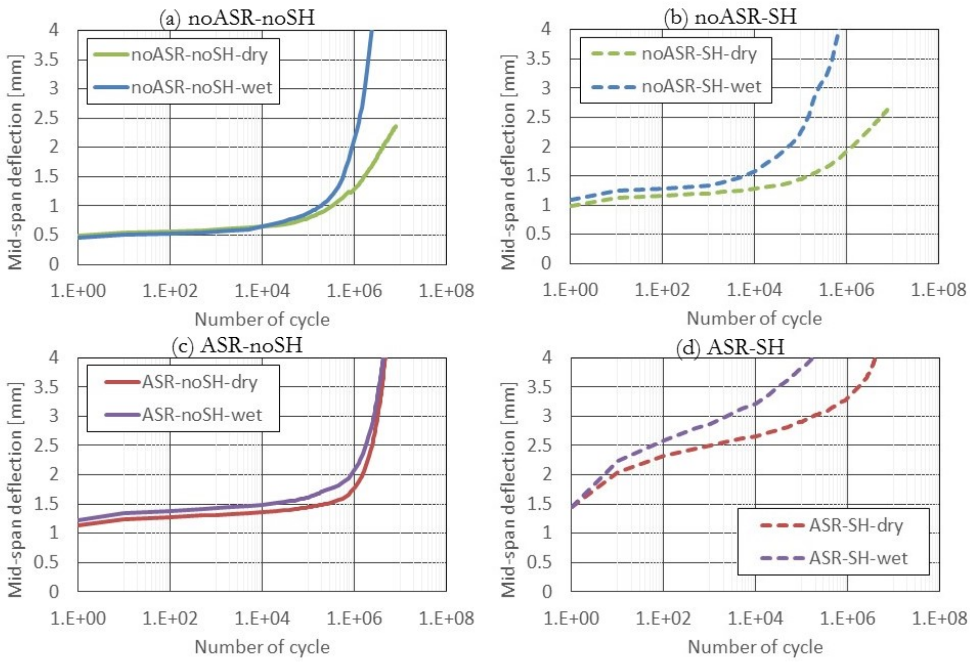

FIGURE 10: Simulated water effect on the fatigue life

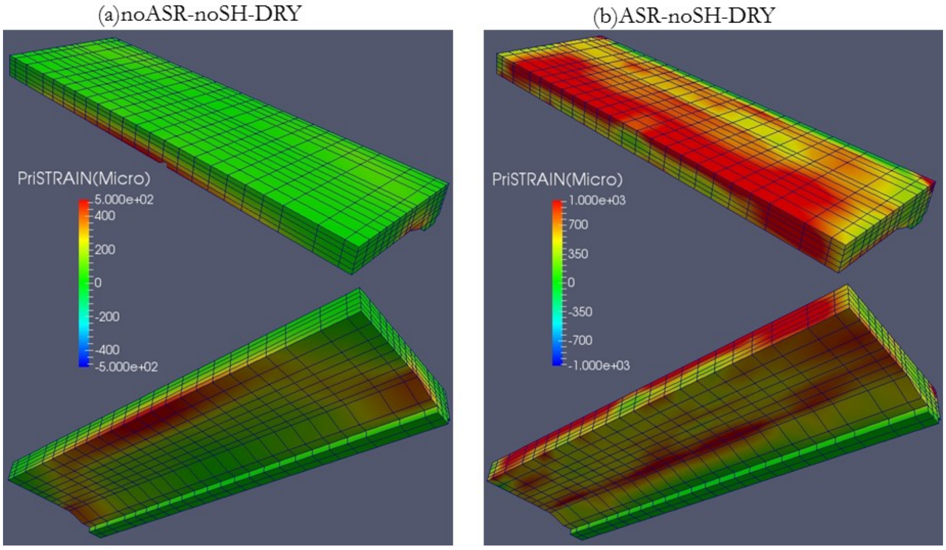

FIGURE 11: Principal strain distributions

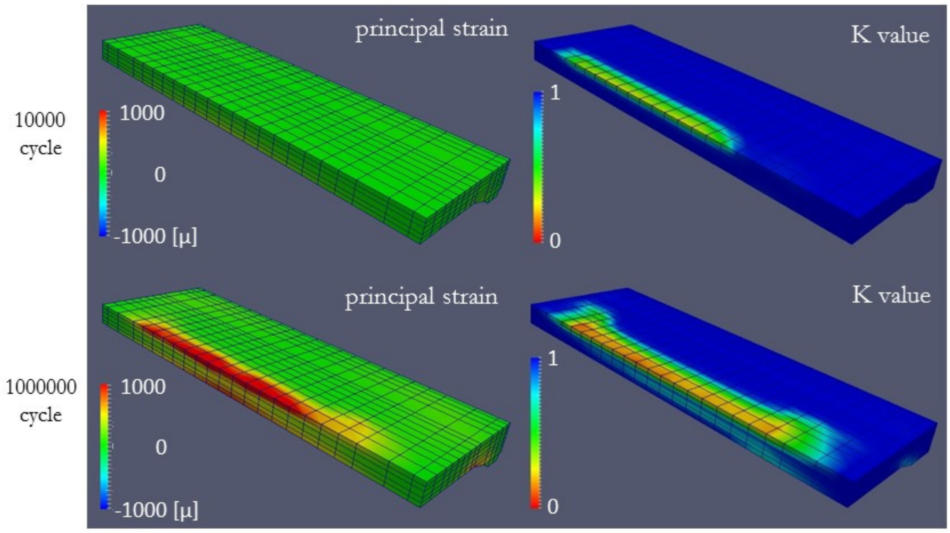

FIGURE 12: Strain distribution and K value distribution for noASR-noSH-WET case

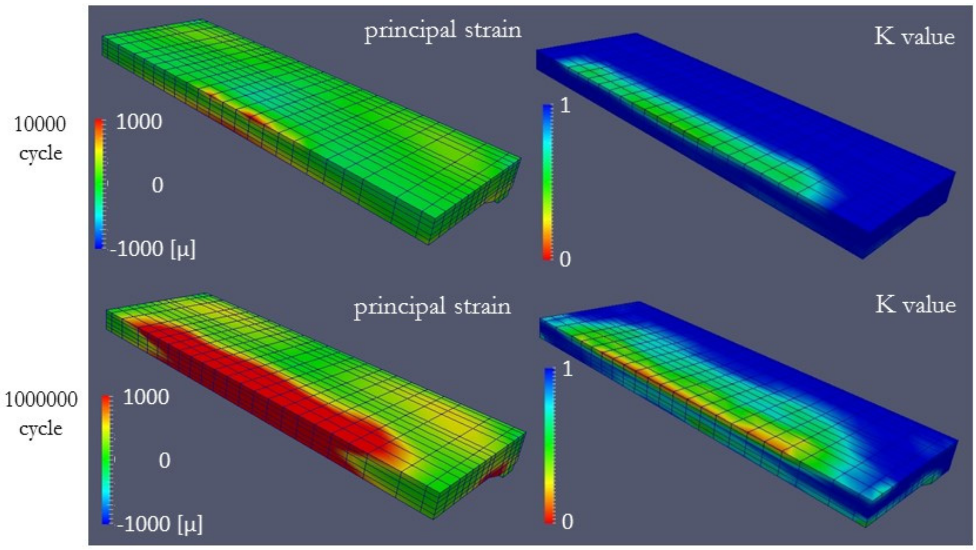

FIGURE 13: Strain distribution and K value distribution for noASR-SH-WET case

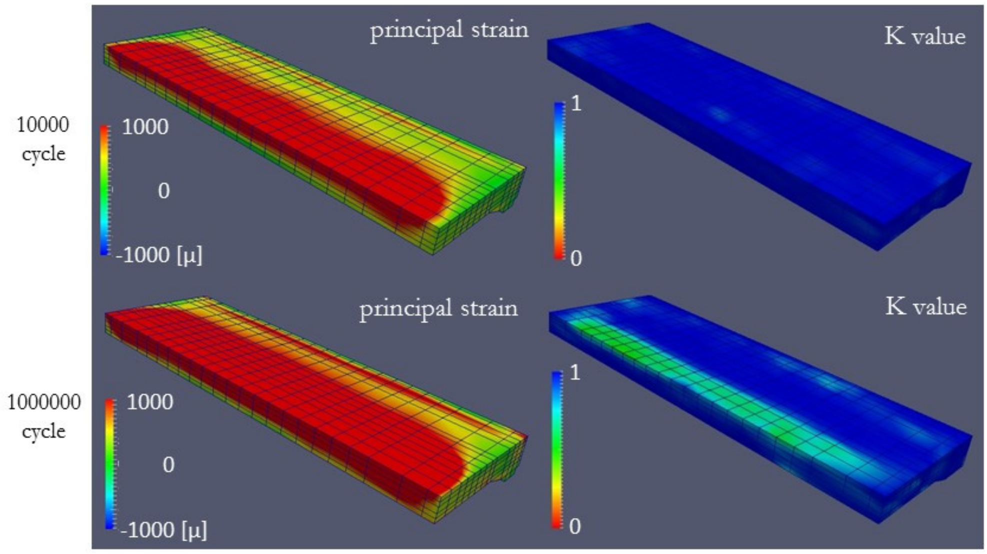

FIGURE 14: Strain distribution and K value distribution for ASR-noSH-WET case

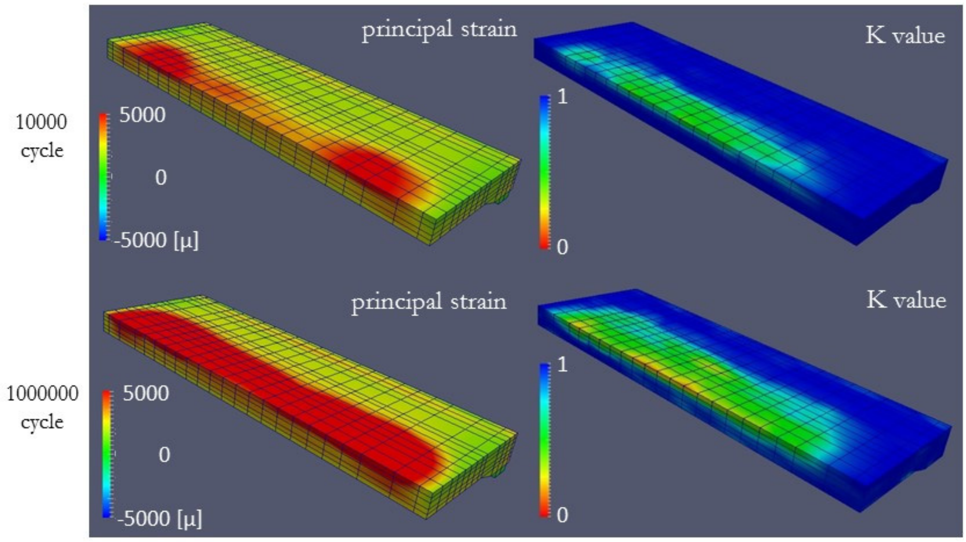

FIGURE 15: Strain distribution and K value distribution for ASR-SH-WET cases

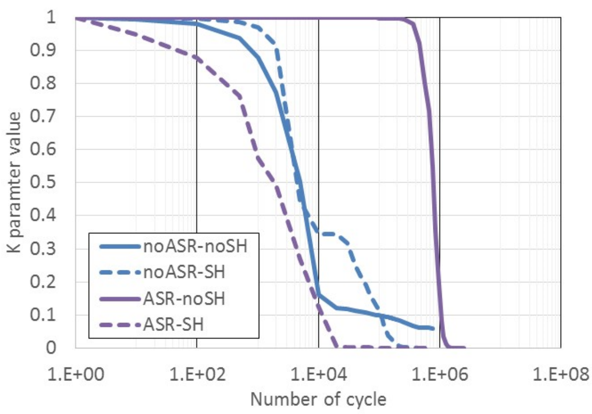

FIGURE 16: Transition of K value at point of top surface of mid span